*Int. J. Electrochem. Sci.*, 14 **(2019)** 3740 – 3751, doi: 10.20964/2019.04.11

International Journal of
ELECTROCHEMICAL
SCIENCE
www.electrochemsci.org

# Preparation and Properties of an Electroless Triple-Layered Ni-P Based-$TiO_2$/$ZrO_2$ Composite Coating

*Qin-Ying Wang, Shuang Liu, Yi-Rong Tang, Rui Pei, Yu-Chen Xi*[*], *Dai-Xiong, Zhang*

School of Materials Science and Engineering, Southwest Petroleum University, Chengdu 610500, China
[*]E-mail: wangqy0401@pku.edu.cn

*Received:* 27 November 2018 / *Accepted:* 11 January 2019 / *Published:* 10 March 2019

We first reported here a new triple-layered Ni-P based-$TiO_2$/$ZrO_2$ (NTZ) composite coating prepared by electroless plating on a substrate of Q235 carbon steel. The microstructure, mechanical and anticorrosion properties of the achieved coating were investigated. Meanwhile, a pure Ni-P coating, a double-layered Ni-P based-$TiO_2$ coating (NT) and a Ni-P based-$ZrO_2$ coating (NZ) were prepared as comparisons. The results indicated that $TiO_2$ and $ZrO_2$ particles were found on the surface of NT and NZ. Both types of the particles were detected on the cross-section of NTZ. In addition, NTZ not only showed a higher tribology property than other coatings but also a similar hardness with NZ. Furthermore, the highest corrosion resistance of NTZ among all coatings was determined by the lowest corrosion current density of $3.80\times10^{-7}$ A/cm$^2$. Ni-P/$TiO_2$ layer under Ni-P/$ZrO_2$ layer in NTZ caused a higher corrosion resistance than NZ by increasing the corrosion path of harmful ions to substrate. The above research revealed that NTZ owned a potential application in the fields requiring both high mechanical and anticorrosion properties.

**Keywords:** Ni-P based-$TiO_2$/$ZrO_2$ composite coating; Electroless plating; Hardness; Tribology property; Corrosion resistance

## 1. INTRODUCTION

Carbon steels are widely applied in industries because of low cost and satisfactory mechanical properties. However, a harsh environment usually causes carbon steels serious corrosion. Electroless plating is a cost-effective method to prepare a high corrosion and wear resistant Ni-P coating on the substrate of a carbon steel [1, 2]. However, the mechanical properties of the pure Ni-P coating still need further improvement by heat treatment or particle strengthening for better application. Heat treatment shows a benefit to enhance the mechanical properties, while may decrease the corrosion resistance of the Ni-P coating due to the transition of the amorphous structure to the crystalline structure. In contrast, particle strengthening can not only enhance the mechanical properties but also

help improve the corrosion resistance of the Ni-P coating, and thus is extensively applied to refine its performance. The corrosion-improved efficiency mainly depends on the types of particles. In recent decades, Ni-P based-nano/micro particle composite coatings have been widely developed as the increasing need for the high quality and multifunctional coatings [1, 3]. For example, composite coatings Ni-P-SiC (SiC: 5 ~ 15 g/L, hardness: 510 ~ 580 $HV_{0.05}$) [4], Ni-P-WC (WC: 3 ~ 12 g/L, hardness: 460 ~ 630 $HV_{0.05}$) [5], Ni-P-$ZrO_2$ ($ZrO_2$: 0~90 g/L, hardness: 550 ~ 1100 $HV_{0.1}$) [6], Ni-MWCNT (MWCNT: 0.1 ~ 0.4 g/L, hardness: 372 ~ 921 $HV_{0.05}$) [7], etc. were developed to enhance the mechanical properties of the pure Ni-P coating [8]. Ni-P-$TiO_2$ ($TiO_2$: 1~10 g/L, corrosion current density ($I_{corr}$): 6.60 μA/cm$^2$) [9], Ni-P-Mo (Mo: ~ 2 wt. %, $I_{corr}$: 13 μA/cm$^2$) [10], Ni-Co-P-$Al_2O_3$ ($Al_2O_3$: ~ 4 wt. %, $I_{corr}$: $2.9\times10^{-5}$ μA/cm$^2$) [11], etc. were also prepared to improve the corrosion resistance of the pure Ni-P coating. Among the above particles, $TiO_2$ and $ZrO_2$ were widely employed in the electroless Ni-P coating to improve both mechanical and anticorrosion properties. Novakovic [12] found that the addition of $TiO_2$ particles (200-300 nm) in Ni-P coating slightly increased corrosion resistance, while the hardness of the heated Ni-P-$TiO_2$ composite coating was higher than that of the heated pure Ni-P coating. Meanwhile, smaller size $TiO_2$ particles (25 nm) were reported to largely enhance the mechanical and anti-corrosion properties of the pure Ni-P coating. Both properties were further improved by increasing the content of $TiO_2$ particles in plating solution [13]. The similar effect of $ZrO_2$ (10-30 nm) particles was found by Song [14] and Wang [15]. In addition, the efficiency of nano $TiO_2$ particles to increase the corrosion resistance of Ni-P coating seemed higher than that of $ZrO_2$ particles, while that to enhance mechanical properties was opposite for the two particles by comparing the relevant literature [13, 14]. This phenomenon indicates that the mechanical and anti-corrosion properties can be improved to a satisfied value simultaneously by using both $TiO_2$ and $ZrO_2$ particles. Actually, Ni-P based composite coatings with the mixed two types of particles have been tried, e.g. Ni-P-PTFE-SiC [16], Ni-P- (mixed) $RuO_2$/$TiO_2$ [17] and Ni-P-Ag-$Al_2O_3$ [18]. However, most of them mainly focused on increasing mechanical properties or oxidation resistance. In addition, the inter-influence between the two types of particles cannot be avoided during plating, which will reduce the properties of composite coatings. Based on the above analysis, a study on electroless Ni-P based composite coatings with two separated layers was developed to improve both mechanical and anticorrosion properties, the high hardness of $ZrO_2$ particle and the excellent anticorrosion property of $TiO_2$ particle make them the suitable candidate for this purpose, which was rare reported.

In this study, we tried to improve the mechanical and anticorrosion properties of Ni-P coating by adding $TiO_2$ and $ZrO_2$ particles, and thus a Ni-P based-$TiO_2$/$ZrO_2$ triple-layered composite coating was developed. Then, the performance of the achieved coating was studied, which was also compared with those of pure Ni-P, double-layered Ni-P based-$TiO_2$, and Ni-P based-$ZrO_2$ coatings.

## 2. MATERIALS AND METHOD

### *2.1 Materials*

A triple-layered Ni-P based-$TiO_2$/$ZrO_2$ composite coating was prepared by the method of electroless plating. The composition of the plating solution is determined by considering the basic mechanism of electroless plating and a long-term experience, as shown in Table 1. Among the above

chemicals, $NiSO_4 \cdot 6H_2O$ was the source of nickel for Ni-P coating; $NaH_2PO_2 \cdot H_2O$ worked as reducing agent to promote the reactions of $H_2PO^{2-} + H_2O \rightarrow HPO_3^{2-} + H^+ + 2H$ and $H_2PO^{2-} + H \rightarrow H_2O + OH^- + P$ to help form Ni-P coating; $C_2H_3O_2Na$ worked as complexing agent to control the rate of reaction; $CH_4N_2S$ was a stabilizer to make plating solution stable; $C_6H_8O_7 \cdot H_2O$ was used to adjust the pH of the plating solution; SDS (Sodium dodecyl sulfate) was a surfactant to prevent agglomeration of nano $TiO_2/ZrO_2$ particles.

**Table 1.** Compositions of the plating solution and technological parameters of electroless plating

| plating solution | content/volume | technological parameters |
|---|---|---|
| $NiSO_4 \cdot 6H_2O$ | 20 g/L | - |
| $NaH_2PO_2 \cdot H_2O$ | 24 g/L | - |
| $C_6H_8O_7 \cdot H_2O$ | 8 g/L | - |
| | | pH |
| $C_2H_3O_2Na$ | 10 g/L | 4.0~4.5 |
| $CH_4N_2S$ | 5m g/L | temperature 85±1°C |
| | | stirring speed |
| The mixed solution ($ZrO_2$, ~3 μm) | 20 mL | 200 r/min |
| ($ZrO_2$: 60 g/L, SDS: 10 g/L, deionized water: Bal.) | | - |
| The mixed solution ($TiO_2$, ~25 nm) | 20 mL | - |
| ($TiO_2$: 60 g/L, SDS: 10 g/L, deionized water: Bal.) | | - |

In this work, the Q235 steel (C 0.16, Mn 0.80, Si 0.37, P 0.04, S 0.04, Fe balance) was cut into approximate dimensions of 10 mm×10 mm×4 mm. Prior to the preparation, the surface of steel was grinded with waterproof abrasive papers (1500 grit), polished with corundum powders of 3~5 μm in diameter, and then ultrasonically cleaned in deionized water followed by ethanol and acetone. Next, the surface of the Q235 steel was etched by hydrochloric acid (15 wt. %) by referring the research of Luo [19]. Then, it was quickly rinsed with deionized water and put into plating solution (300 mL) successively. A pure Ni-P layer was achieved on the surface of the steel after 0.5 h, then the mixed solution ($TiO_2$) was gradually added to the stirred plating solution to prepare the second layer of Ni-P/$TiO_2$ for 0.5 h. Next, the achieved Ni-P-Ni-P/$TiO_2$ composite coating was quickly moved to the stirred plating solution with the mixed solution containing $ZrO_2$ particles to prepare the third layer of Ni-P/$ZrO_2$. The preparing time was also 0.5 h. Finally, a triple-layered Ni-P based-$TiO_2/ZrO_2$ composite coating (NTZ) was obtained. Simultaneously, a pure Ni-P coating, a Ni-P based-$TiO_2$ coating, and a Ni-P based-$ZrO_2$ coating were prepared as comparisons. The preparing details of all the above coatings were summarized in Table 2. The constant temperature magnetic stirrer was used to prepare coatings.

**Table 2.** Preparing details of pure Ni-P, Ni-P based-$TiO_2$, Ni-P based-$ZrO_2$ and Ni-P based-$TiO_2/ZrO_2$ coatings

| Coatings | Plating time |
|---|---|
| Ni-P | NiP: 1 h |
| NT | NiP: 0.5 h + $TiO_2$: 1 h |
| NZ | NiP: 0.5 h + $ZrO_2$: 1 h |
| NTZ | NiP: 0.5 h + $TiO_2$: 0.5 h + $ZrO_2$: 0.5 h |

*2.2. Method*

A scanning electron microscope (SEM, EV0 MA15 ZEISS) equipped with an energy-dispersive X-ray spectrometer (EDS) was applied to observe the morphology and measure the elemental composition of coatings. An X-ray diffractometer (XRD, X Pert PRO MPD) was used to measure the phase compositions of coating at a scanning range of 0 ° to 60 °. A Vickers hardness tester (HXD-2000TM/LCD, Baoleng) was employed to test the hardness of coating surface under a load of 0.98 N and a dwell time of 15 s. A multifunctional scratching tester (MFT-4000) with a diamond indenter was used to measure the friction coefficients of coatings under a scratching speed of 5 mm/min and a gradually varied force of 0 ~ 10 N.

Electrochemical tests were carried out in 3.5 wt. % NaCl solution by an electrochemical workstation (CS310, Corrtest) at room temperature. The electrochemical impedance spectroscopy (EIS) was measured at a frequency range from 100 kHz to 10 MHz with an applied AC amplitude of 10 mV. The potentiodynamic polarization curve of the coating was tested at stable open circuit potential (OCP) achieved after the immersion time of 2 h with a potential scanning rate of 1 mV/s. A conventional three-electrode cell, containing a saturated calomel electrode (SCE) as the reference electrode, a platinum electrode as the counter electrode and the coating with an exposed surface area of 10 mm × 10 mm as the working electrode, was employed.

## 3. RESULTS AND DISCUSSION

*3.1 Microstructure and composition*

The morphologies and corresponding EDS spectra of the achieved coatings are shown in Figure 1. It can be seen that the surfaces of all coatings are uniform. Small particles of NT, NZ, and NTZ are found on the surfaces. Moreover, NZ and NTZ display the similar surface morphology because they both demonstrate a Ni-P/$ZrO_2$ layer on the top surface. EDS results presented in Figure 1 e-h and summarized in Table 3 provide the elemental compositions of coatings. It is noted that only Ni and P are found at the surface of the pure Ni-P coating. Whereas, extra Ti and Zr are observed at the surfaces of NT and NZ/NTZ with the contents of 4-5 wt. % and 8-10 wt. %, respectively. This result indicates the successful preparation of composite coatings. In addition, the presence of $ZrO_2$ or $TiO_2$ particles in the bath seems to increase the P content in the composite coatings. This result is similar to Novakovic [20].

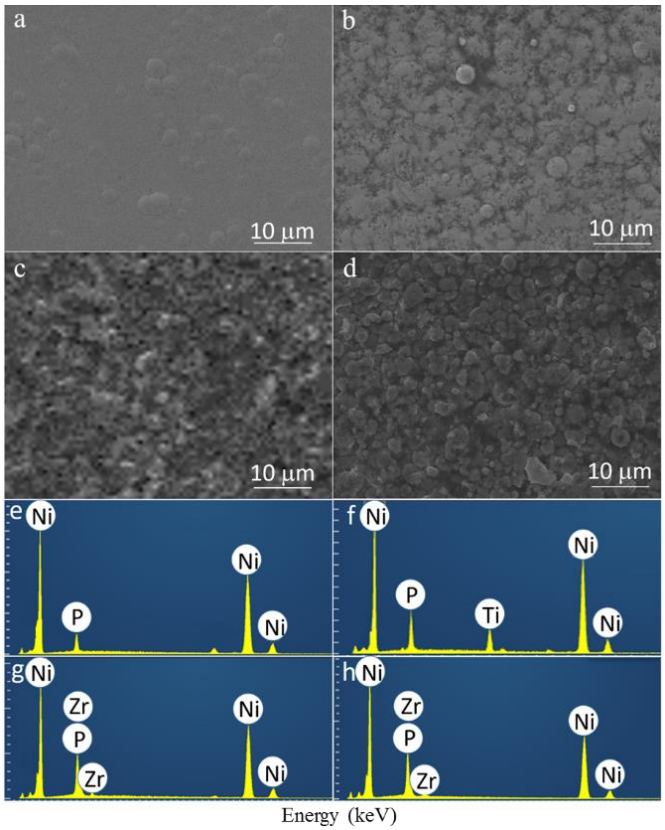


**Figure 1.** SEM micrographs and EDS map scanning results of coatings, a/e: pure Ni-P; b/f: Ni-P based-$TiO_2$; c/g: Ni-P based-$ZrO_2$; d/h: Ni-P based-$TiO_2$/$ZrO_2$

**Table 3**. Contents of elements on the pure Ni-P, Ni-P based-$TiO_2$, Ni-P based-$ZrO_2$ and Ni-P based-$TiO_2$/$ZrO_2$ coatings surface

| Coating | Ni-P | NT | NZ | NTZ |
|---|---|---|---|---|
| O (wt. %) | - | 3.94 | 3.7 | 2.8 |
| P (wt. %) | 14.95 | 16.72 | 18.58 | 17.75 |
| Ni (wt. %) | 82.90 | 71.58 | 65.61 | 67.4 |
| Zr (wt. %) | - | - | 8.73 | 9.4 |
| Calculated $ZrO_2$ (wt. %) | - | - | 11.8 | 12.7 |
| Ti (wt. %) | - | 4.31 | - | - |
| Calculated $TiO_2$ (wt. %) | - | 7.20 | - | - |

The cross-sectional morphologies of achieved coatings are displayed in Figure 2. It can be seen that the thickness of Ni-P layer between steel substrate and the composite coating is around 10 μm. Meanwhile, the thicknesses of all coatings are around 13 μm although the deposited time for pure Ni-P and other composite coatings are different, i.e. 1 h for the former, while 2 h for the latter. This phenomenon indicates that the addition of particles reduces the plating rate of Ni-P coating. It is ascribed to the decrease of the active area on the surface caused by the blocking of particles. In addition, the Ni-P/$TiO_2$ layer in NT, the Ni-P/$ZrO_2$ layer in NZ and the Ni-P/$TiO_2$/$ZrO_2$ double layer in

NTZ show the similar thicknesses around 3 μm. Meanwhile, Ni-P/$TiO_2$/$ZrO_2$ double layer in NTZ is composed of a Ni-P/$TiO_2$ layer and a Ni-P/$ZrO_2$ layer with the similar thickness of 1.5 μm. The white arrows and lines, as seen in Figure 2 b-d denote the different layers of the composite coatings. Additionally, the interfaces between all coatings and the corresponding substrates are clear and well-bonded, and the achieved coatings were uniform, compact, pore free, revealing satisfactory quality. These results are in accordance with those of Song [14].

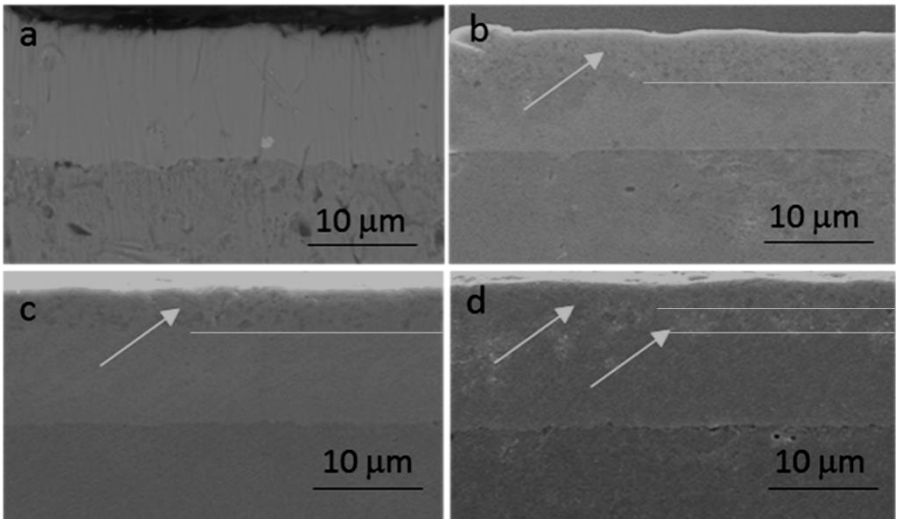


**Figure 2.** Cross-sectional SEM morphology of coatings, a: pure Ni-P; b: Ni-P based-$TiO_2$; c: Ni-P based-$ZrO_2$; d: Ni-P based-$TiO_2$/$ZrO_2$

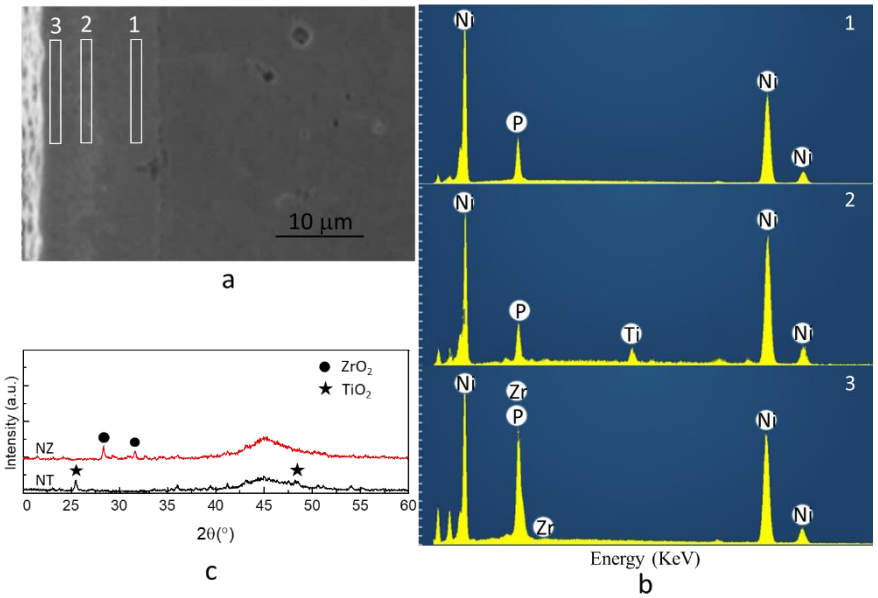


**Figure 3.** SEM image of cross-section of Ni-P based-$TiO_2$/$ZrO_2$ (a), and the EDS results within the regions 1, 2 and 3 at cross-section of Ni-P based-$TiO_2$/$ZrO_2$ (b), and the XRD patterns of Ni-P based-$TiO_2$ and Ni-P based-$ZrO_2$ (c)

The EDS at regions 1, 2 and 3 along the cross-section of NTZ was tested and provided in Figure 3 to confirm the deposition of $TiO_2$ and $ZrO_2$ particles in NTZ. It is noted that except Ni and P,

Zr and O are found on the top surface of NTZ, Ti and O are observed at region 2, while only Ni and P are found at region 1. The comparative results reveal that NTZ is composed of a Ni-P/$ZrO_2$ layer, a Ni-P/$TiO_2$ layer, and a Ni-P layer connecting each other from top surface to the steel substrate. In addition, the XRD patterns of NT and NZ were measured and provided in Figure 3 c. The characteristic peaks of $TiO_2$ and $ZrO_2$ are found by comparing the standard PDF cards in the XRD patterns of NT and NZ, respectively, indicating the successful deposition of the $TiO_2$ or $ZrO_2$ particles in each coating.

### *3.2 Mechanical property*

In order to learn about the effects of particles on the mechanical properties of electroless coatings, the hardness was tested and provided in Figure 4. The results reveal that the double-layered coatings exhibit the enhanced hardness as compared to that of pure Ni-P. This result is similar to the study of Makkar [21] and Gay [22]. In addition, the hardness of NZ is larger than that of NT. Efficient influence on enhancing hardness based on dispersion hardening by the additions of $ZrO_2$ than $TiO_2$ particles has been well illustrated [23, 24]. In addition, the Ni-P/$ZrO_2$ layer with the thickness of 1.5 μm on NTZ surface displays the similar hardness above 712 $HV_{0.1}$ with the Ni-P/$ZrO_2$ layer of 3 μm on NZ. This phenomenon is attributed to the supportive effect of Ni-P/$TiO_2$ layer under Ni-P/$ZrO_2$ layer of NTZ. It means that the addition of $TiO_2$ particles did not worsen the hardness of the triple-layered NTZ compared with NZ.

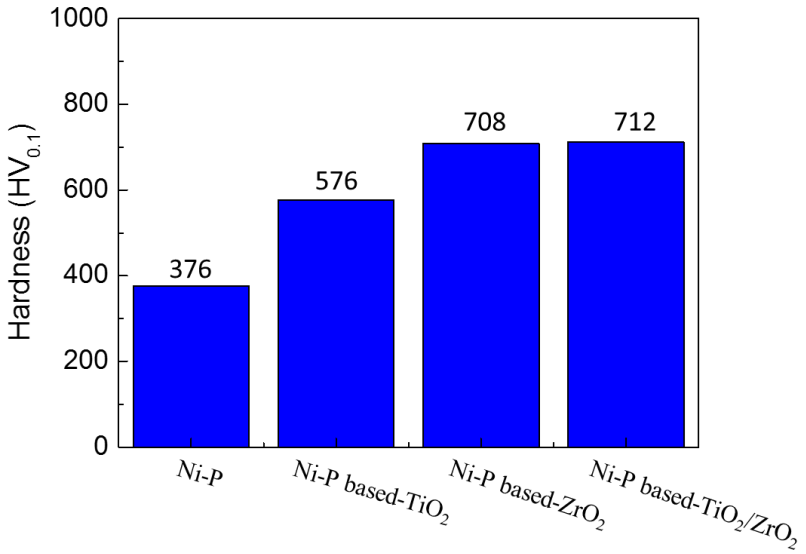


**Figure 4.** Vickers hardness of pure Ni-P, Ni-P based-$TiO_2$, Ni-P based-$ZrO_2$ and Ni-P based-$TiO_2$/$ZrO_2$ coatings

The friction coefficients with corresponding variation trend were provided in Figure 5 to evaluate the tribology property of coatings. The scratching speed of indenter is a constant (5 mm/min) during the experiment, and thus the lateral force at surface remains unchanged. It means that the friction coefficient will increase as improving normal force [25]. The same trend of friction coefficients versus increasing normal force was found for all coatings, as displayed in Figure 5

Furthermore, pure Ni-P and NT display friction coefficients of 0.24 and 0.16 at 10 N, respectively, which are larger than those of NZ and NTZ with the values around 0.1, which indicates that hard $ZrO_2$ particles are beneficial to reduce the friction coefficient and improve the tribology property. Additionally, NTZ displays a slightly lower friction coefficient than NZ, revealing higher tribology property. This is mainly ascribed to the supportive effect of Ni-P/$TiO_2$ layer under Ni-P/$ZrO_2$ layer when NTZ was damaged by the indenter [26].

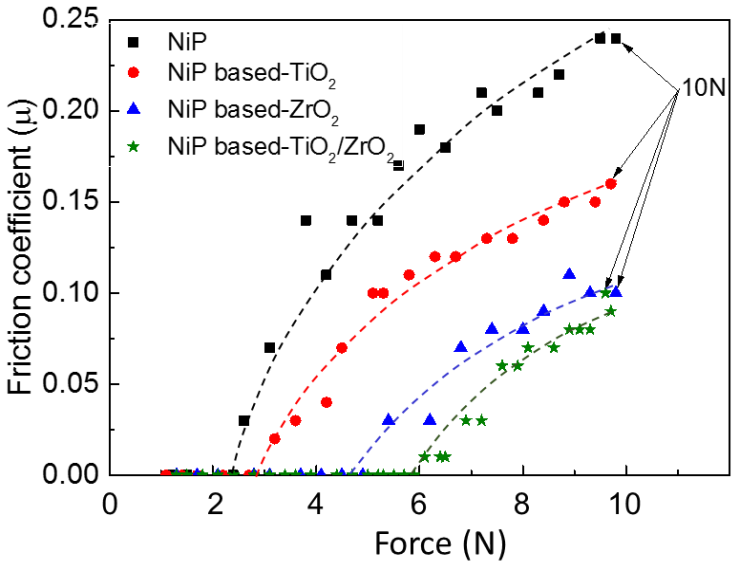


**Figure 5.** Friction coefficients of pure Ni-P, Ni-P based-$TiO_2$, Ni-P based-$ZrO_2$ and Ni-P based-$TiO_2$/$ZrO_2$ coatings

*3.3 Corrosion behavior and mechanism*

The EIS of coatings was done for determining whether NTZ owns the advantage in the field of corrosion prevention, as shown in the Figure 6. It is found that all coatings display one depressed capacitive loop within the whole frequency range. The radius of the capacitive loop from large to small is in the order of NTZ, NT, NZ and pure Ni-P, indicating decreasing corrosion resistance accordingly.

The potentiodynamic polarization curves of coatings were tested and presented in Figure 7. It can be seen that NTZ exhibits the lowest anodic polarization current density among all coatings, revealing a reduced corrosion. In addition, the corrosion current density ($I_{corr}$) was calculated by the electrochemical system through linearly fitting the strongly polarized regions (|over potential| $\geq$ 100 mV) of the anodic and cathodic curves [27]. Consequently, $I_{corr}$ is $4.78\times10^{-7}$ A/cm$^2$, $1.03\times10^{-6}$ A/cm$^2$ and $3.80\times10^{-7}$ A/cm$^2$ for NT, NZ, and NTZ accordingly, all of which are lower than that of pure Ni-P coating with the $I_{corr}$ of $1.18\times10^{-6}$ A/cm$^2$ as shown in Table 4. The research of Ma [28] found that the Ni-P-$TiO_2$ and Ni-P-$ZrO_2$ composite coatings have high corrosion resistance that Ni-P coating. This result is in accordance with this study. The lower $I_{corr}$ of NTZ compared with NT indicates a lower corrosion rate.

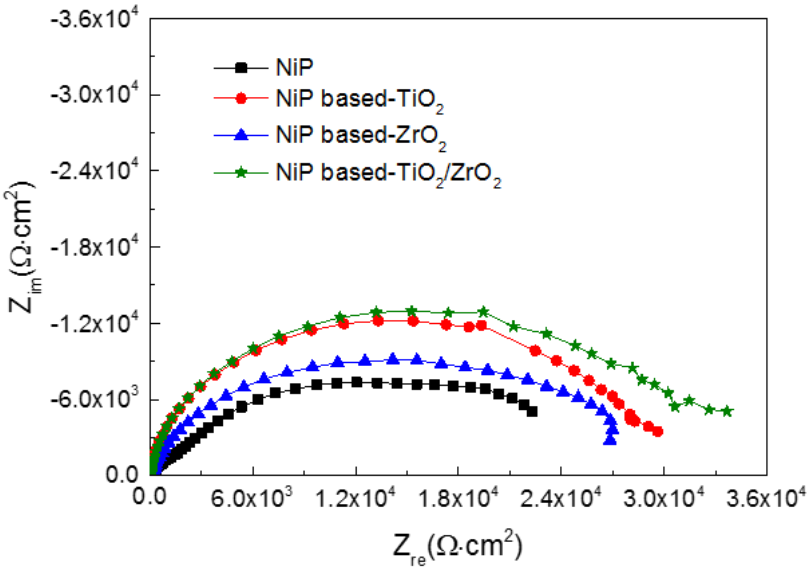


**Figure 6.** Nyquist plots of pure Ni-P, Ni-P based-$TiO_2$, Ni-P based-$ZrO_2$ and Ni-P based-$TiO_2$/$ZrO_2$ coatings in 3.5 wt. % NaCl solution.

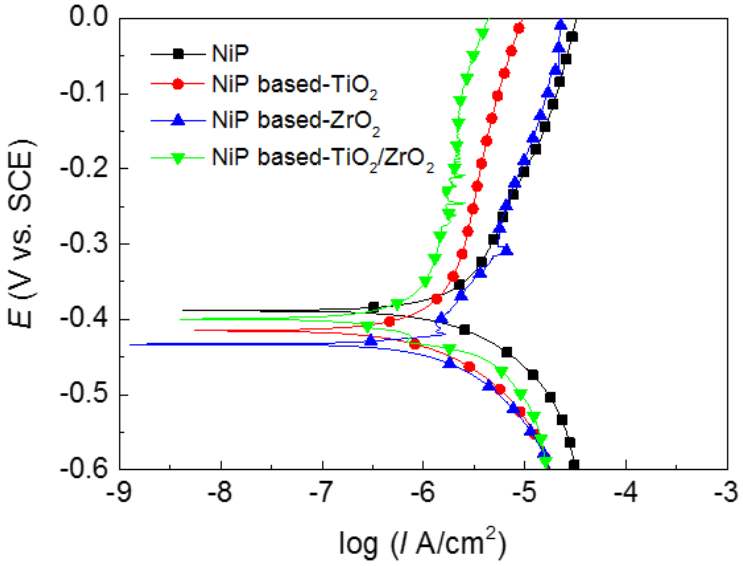


**Figure 7.** Potentiodynamic polarization curves of pure Ni-P, Ni-P based-$TiO_2$, Ni-P based-$ZrO_2$ and Ni-P based-$TiO_2$/$ZrO_2$ coatings in 3.5 wt. % NaCl solution

**Table 4.** Corrosion potential ($E_{corr}$) and corrosion current density ($I_{corr}$) of pure Ni-P, Ni-P based-TiO2, Ni-P based-$ZrO_2$ and Ni-P based-$TiO_2$/$ZrO_2$

| Coating | Ni-P | NT | NZ | NTZ |
|---|---|---|---|---|
| $E_{corr}$ (V) | -0.381 | -0.425 | -0.431 | -0.401 |
| $I_{corr}$ (A/cm$^2$) | $1.18\times10^{-6}$ | $4.78\times10^{-7}$ | $1.03\times10^{-6}$ | $3.8\times10^{-7}$ |

The corrosion mechanism of coatings is demonstrated in Figure 8 by referring to the relevant research regarding Ni-P-WC electroless coating reported by Luo [19]. For pure Ni-P coating, its

amorphous structure is usually difficult to be corroded for the absences of sensitive sites, i.e. grain boundaries, dislocations, and second-phase precipitates [29]. However, the possible uneven distribution of P on the surface of Ni-P coating during electroless plating will lead to micro-galvanic cells. As a result, the dynamic balance of Ni <—> $Ni^{2+}$ + $2e^-$ will be destroyed and the soluble $NiCl_2$ formed through the reaction of $Ni^{2+}$ + $2Cl^-$ <—> $NiCl_2$ will cause pitting corrosion [30], as shown in Figure 8 a. Fortunately, the above mechanism is changed by co-depositing particles of $TiO_2$ and $ZrO_2$ in coatings NT, NZ and NTZ. For one aspect, the presence of particles will prevent the gather of Ni or P, thus helps obtain a composite coating with a uniform matrix. This composite structure will lead to fewer galvanic cells to worsen corrosion. For another aspect, the oxide particles will act as barriers to block and prolong the corrosion path into the coating, which will further reduce corrosion, as schematically shown in Figure 8 b-d. Whereas, the difference in the types and concentrations of oxide particles will cause a slightly different corrosion mechanism for double-layered and triple-layered coatings. First, the volume fraction of $ZrO_2$ in composite coatings is higher than that of $TiO_2$, which is calculated by the ratio of the mass fraction (Table 3) and the density. The calculated volume fractions of $ZrO_2$ and $TiO_2$ particles in composite coatings are 1.43-1.7% and 0.93-1.16%, respectively. However, the particle size of $TiO_2$ (25 nm) is much smaller than that of $ZrO_2$ (3 μm), indicating a larger surface area. Therefore, the effect of $TiO_2$ particles to block corrosion path is more efficient than that of $ZrO_2$ particles. Meanwhile, smaller $TiO_2$ particles will be in favor of forming a more compact structure. It is the reason why NT displays higher corrosion resistance than NZ, as presented in Figure 8 b-c. Furthermore, $ZrO_2$ particles on the outer layer of NTZ mainly act as barriers to block harmful $Cl^-$ to penetrate into the under Ni-P/$TiO_2$ layer, while the Ni-P/$TiO_2$ layer show the similar corrosion resistance as that in NT. As a result, the combined effects of both Ni-P/$ZrO_2$ and Ni-P/$TiO_2$ layers for NTZ cause a higher corrosion resistance than NT, as shown in Figure 8 b, d. In addition, the nethermost Ni-P layer will display serious corrosion once the upper layers, i.e. Ni-P/$ZrO_2$ or/and Ni-P/$TiO_2$, are damaged.

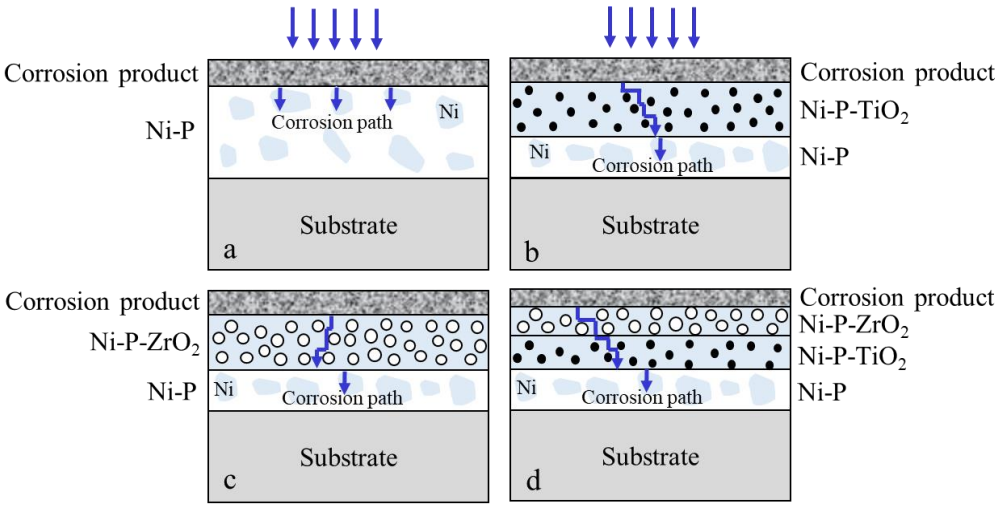


**Figure 8.** Corrosion mechanisms of pure Ni-P, Ni-P based-$TiO_2$, Ni-P based-$ZrO_2$ and Ni-P based-$TiO_2$/$ZrO_2$ in 3.5 wt. % NaCl solution.

Generally, the electroless plating method has got better mechanical and anticorrosion properties with uniform and well-connected triple-layer system. Clearly, the current method to prepare the triple-layered coating is relatively complex, which requires electroless plating for at least two times, and thus this procedure needs to be further optimized. In addition, the study on the performance of the achieved coating in a real serving environment should be conducted before we can make confident statements on its practical application value.

## 4. CONCLUSIONS

A triple-layered NTZ composite coating was prepared by the method of electroless plating. The results showed the uniform morphology of NTZ containing $ZrO_2$ particles in the top layer and $TiO_2$ particles in the second layer. In addition, NTZ not only displayed the similar hardness as NZ but also showed a better tribology property than pure Ni-P and other coatings. Meanwhile, the highest corrosion resistance was found for NTZ with the lowest corrosion current density of $3.80\times10^{-7}$ A/cm$^2$. $ZrO_2$ particles to block corrosion path in the top layer and $TiO_2$ particles to cause a compact microstructure in the second layer of NTZ were believed the main reasons. The above research indicated that the achieved triple-layered Ni-P based-$TiO_2$/$ZrO_2$ coating exhibited the advantages in both mechanical and anticorrosion properties.

ACKNOWLEDGEMENT
This research was financially supported by Young Elite Scientists Sponsorship Program by China Association for Science and Technology (YESS, CAST) and Youth Scientific and Innovation Research Team for Advanced Surface Functional Materials, Southwest Petroleum University (No. 2018CXTD06).

## References

1. J. Sudagar, J. Lian, W. Sha, *J. Alloy. Compd*., 571 (2013) 183.
2. J. Ru, Y. Jia, Y. Jiang, J. Feng, R. Zhou, Y. Hua, D. Wang, *Surf. Eng*., 10 (2016) 1.
3. M. Sarret, C. Muller, A. Amell, *Surf. Coat. Tech*., 201 (2006) 389.
4. J. Gao, L. Liu, Y. Wu, B. Shen, W. Hu, *Surf. Coat. Tech*., 200 (2006) 5836.
5. C. Zhao, Y. Yao, *J. Mater. Eng. Perform*., 23 (2014) 193.
6. P.A. Gay, J.M. Limat, P.A. Steinmann, J. Pagetti, *Surf. Coat. Tech*., 202 (2007) 1167.
7. A. Selvakumar, R. Perumalraj, P. Jeevananthan, S. Archana, J. Sudagar, *Surf. Eng*., 32 (2016) 338.
8. H. Liu, H.L. Yao, G.E. Thompson, Z. Liu, G. Harrison, *Surf. Eng*., 31 (2015) 412.
9. S.R. Allahkaram, S. Salmi, E. Tohidlou, *Int. J. Mod. Phys.: Conference Series*., 5 (2012) 833.
10. A.E. Fetohi, R.A. Hameed, K.M. El-Khatib, *J. Power Sources*., 240 (2013) 589.
11. J. Hu, L. Fang, X.L. Liao, L.T. Shi, *Surf. Eng*., 27 (2016) 1.
12. J. Novakovic, P. Vassiliou, K. Samara, T. Argyropoulos, *Surf. Coat. Tech*., 201 (2006) 895.
13. M. Momenzadeh, S. Sanjabi, *Mater. Corros*., 63 (2015) 614.
14. Y.W. Song, D.Y. Shan, R.S. Chen, E.H. Han, *Surf. Eng*., 23 (2007) 334.
15. Y. Wang, X. Shu, S. Wei, C. Liu, W. Gao, R.A. Shakoor, R. Kahraman, *J. Alloy. Compd*., 630 (2015) 189.
16. Y.S. Huang, X.T. Zeng, I. Annergren, F.M. Liu, *Surf. Coat. Tech*., 167 (2003) 207.
17. J. Novakovic, P. Vassiliou, E. Georgiza, *Int. J. Electrochem. Sci*., 8 (2013) 3615.

18. S. Alirezaei, S.M. Monirvaghefi, A. Saatchi, M. Ürgen, K. Kazmanli, *Tribol. Int*., 62 (2013) 110.
19. H. Luo, M. Leitch, Y. Behnamian, Y. Ma, H. Zeng, J.L. Luo, *Surf. Coat. Tech*., 277 (2015) 99.
20. J. Novakovic, M. Delagrammatikas, P. Vassiliou, C.T. Dervos, *Defect. Diffus. Forum*., 297-301 (2010) 899.
21. P. Makkar, R.C. Agarwala, V. Agarwala, *Adv. Powder. Tech*., 25 (2014) 1653.
22. P.A. Gay, J.M. Limat, P.A. Steinmann, J. Pagetti, *Surf. Coat. Tech*., 202 (2007) 1167.
23. Y. Yang, W. Chen, C. Zhou, H. Xu, W. Gao, *Appl. Nanosci*., 1 (2011) 19.
24. X. Wu, J. Mao, Z. Zhang, Y. Che, *Surf. Coat. Tech*., 270 (2015) 170.
25. S. Skolianos, T.Z. Kattamis, *Mat. Sci. Eng. A-Struct*., 163 (1993) 107.
26. Q.H. Wang, Q.J. Xue, H.W. Liu, W.C. Shen, J.F. Xu, *Wear*., 198 (1996) 216.
27. C.N. Cao, Principles of Electrochemistry of Corrosion, Chemical Industry Press, (2008) Beijing, China.
28. M.H. Ma, X.H Li, Y. Shan, *Surf. Tech*., 35 (2006) 45.
29. C.A. Souza, D.V. Ribeiro, C.S. Kiminami, *J. Non-Cryst. Solids*., 442 (2016) 56.
30. Y.W. Song, D.Y. Shan, E.H. Han, *Electrochim. Acta*., 53 (2007) 2009.